Structure and Photoinduced Excited State Keto−Enol Tautomerization of 7-Hydroxyquinoline-$(CH_3OH)_n$ Clusters

Yoshiteru Matsumoto, Takayuki Ebata,* and Naohiko Mikami

Department of Chemistry, Graduate School of Science, Tohoku University, Sendai 980-8578, Japan

Received: January 16, 2002; In Final Form: April 1, 2002

An investigation on the structures and the excited-state proton-transfer reaction has been carried out for size-selected 7-hydroxyquinoline(7HQ)-methanol hydrogen-bonded clusters in supersonic jets. The structures of the clusters were determined based on the analysis of the fluorescence-detected IR spectra in the OH stretching region and by density functional theory calculations. Two isomers were found to exist for 7HQ-$(CH_3OH)_1$. One has the form in which the OH group of 7HQ is hydrogen-bonded to the oxygen of CH_3OH, and the other has the form in which the OH group of CH_3OH is hydrogen-bonded to the nitrogen of 7HQ. For 7HQ-$(CH_3OH)_2$ and -$(CH_3OH)_3$, their structures were determined to be "enol bridge" form, in which one end of a chain-formed methanol cluster is hydrogen-bonded to the OH group and the other to the nitrogen of 7HQ. Photoinduced excited-state proton-transfer reaction was investigated by measuring the dispersed fluorescence spectra for the clusters. Among them, a visible emission with a maximum at ∼530 nm, which coincides with the tautomer emission of 7HQ generated in methanol solution, was observed for the enol bridge 7HQ-$(CH_3OH)_3$ and larger clusters. This result presents a direct evidence for the enol bridge form 7HQ-$(CH_3OH)_3$ to be a precursor for the proton-transfer reaction in solution.

I. Introduction

Proton transfer is one of the fundamental chemical reactions. Especially, photoinduced proton transfer, so called excited state proton transfer (ESPT), is particularly important both in chemistry and biology. Photoinduced anion formation of aromatic acid such as naphthol in a protic solvent is a typical example of ESPT,[1] in which a large Stokes-shifted visible emission due to the naphtholate anion is observed when ESPT occurs after absorption of the UV light.

The keto↔enol tautomerization of 7-hydroxyquinoline (7HQ), mediated by protic solvent molecules, is another system of ESPT. 7HQ has an OH group acting as a proton donor (acid) and nitrogen acting as a proton acceptor (base). Upon electronic excitation, the OH group becomes more acidic and its proton-donating capability increases, while the nitrogen becomes more basic and increases its proton-accepting capability. Because of the large distance between the OH group and the nitrogen, however, the tautomerization reaction is not likely to occur in isolated condition and is mediated by protic solvent molecules through the multiple proton-transfer reaction.

Mason et al. first observed the dual fluorescence by irradiating 7HQ with UV light in alcohol solution.[2] Since then, various spectroscopic investigations have been carried out for 7HQ in bulk system, such as conventional spectroscopy at room temperature[3−8] and matrix isolation spectroscopy,[9−11] as well as picosecond time-resolved spectroscopy.[5,12−14] Most of the works focused on solving two important problems for the ESPT reaction of 7HQ. The first is to establish how many molecules are needed to promote this reaction and what kind of structure the intermediate species takes, and the second is to determine whether this multiple-proton transfer reaction is a concerted or a stepwise process. It is generally understood that in methanol solution the ESPT reaction occurs when two methanol molecules form bridge-type hydrogen-bonds with 7HQ (Figure 1) from

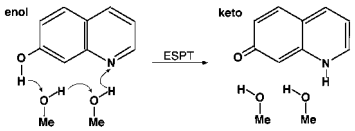

Figure 1. Keto−enol tautomerization scheme of 7HQ with two methanol molecules.

the alcoholic concentration dependence of the absorption spectrum of 7HQ[5,14] and from the result of no visible emission in 8-methyl-substituted 7HQ.[13] Also, several theoretical calculations have been performed to reveal the structure and the reactivity.[15−17] However, up to now there has been no report which directly confirmed the bridge-type structure to be a precursor of the ESPT reaction. It is quite possible that such a species is formed in supersonic jets, and one can obtain the direct evidence that the species is a precursor of the tautomerization reaction.

Several spectroscopic studies on the hydrogen-bonded (H-bonded) clusters of 7HQ have also been reported by using supersonic jets. Laser-induced fluorescence (LIF) and dispersed fluorescence spectra of 7HQ-$(H_2O)_n$ were first reported by Lahmani et al.[18] Bach et al. observed dispersed fluorescence spectra, resonant two-photon ionization (R2PI), and the UV−UV hole-burning spectra of 7HQ-$(H_2O)_n$.[19−21] They proposed an H-bonding structure of 7HQ-$(H_2O)_n$ similar to that shown in Figure 1, from the observed intermolecular vibrations and by ab initio calculations. Though the ESPT reaction was not observed for 7HQ-$(H_2O)_n$ clusters, they recently showed evidence of the ESPT reaction for 7HQ-$(NH_3)_{n\geq 4}$ and reported a possibility of the ground-state intracluster tautomerization reaction for 7HQ-$(NH_3)_{n\geq 7}$.[22]

Most of the studies described above were carried out by using electronic spectroscopy, so there has been no information about the OH stretching vibration which provides us with the most important information on the H-bonded structure.[23−33] Very

10.1021/jp0201128 CCC: $22.00
Published on Web 05/21/2002

recently, we succeeded in observing the IR spectra of the OH stretching vibrations of size-selected 7HQ-$(H_2O)_n$ by using IR−UV double-resonance spectroscopy. From the observed spectra and by use of ab initio calculations, we concluded that 7HQ-$(H_2O)_1$ has two isomers (OH−O and N−HO structures) and that the structures of 7HQ-$(H_2O)_2$ and 7HQ-$(H_2O)_3$ are of bridge form, in which a linear-form water dimer or trimer is bound to the OH hydrogen and the nitrogen atom of 7HQ.[34]

In this study, we report our spectroscopic and theoretical studies on 7HQ-$(CH_3OH)_n$. The main theme of this work is to obtain firm evidence of the bridge-type structure to be a precursor of the ESPT reaction and to determine how many solvent molecules are needed to initiate the reaction. We first present the IR spectra of the OH stretching vibrations of 7HQ-$(CH_3OH)_n$ that are observed by IR−UV double-resonance spectroscopy. The structures are determined from the observed IR spectra and those of the clusters obtained by density functional theory (DTF) calculations. We then examine the intracluster ESPT reaction by observing the dispersed fluorescence (DF) spectra of the above-mentioned clusters. We found that the critical size of the ESPT in 7HQ-$(CH_3OH)_n$ is $n = 3$. The size-dependence of ESPT will be discussed from the difference of the interatomic distances of the calculated structures.

II. Experiment

In the present experiment, we used IR−UV double-resonance spectroscopy with fluorescence detection, so-called fluorescence-detected infrared spectroscopy (FDIRS), to measure the vibrational spectra of size-selected 7HQ-$(CH_3OH)_n$ clusters. The experimental setup for FDIRS was the same as that described elsewhere.[35] The tunable UV and IR light was coaxially introduced into the vacuum chamber in a counterpropagating manner. The two laser beams were focused on a supersonic free jet 15 mm downstream of the nozzle by using lenses (a $f =$ 500 mm lens for UV and a $f = 250$ mm lens for IR). The delay time between the IR and the UV pulses was controlled by a digital delay generator (SRS DG535) with the IR pulse introduced 50 ns prior to UV. The UV frequency was tuned to the S_1-S_0 electronic transition of a particular species, and the fluorescence intensity was monitored, which was the measure of the ground-state population. When the IR frequency was resonant with vibrational transition of the selected species, the ground-state molecules were pumped to the vibrational level, resulting in a depletion of the fluorescence intensity. Thus, the FDIR spectrum was obtained as a fluorescence-dip spectrum by scanning the IR frequency while monitoring the fluorescence signal.

UV−UV spectral hole-burning (SHB) spectroscopy was also carried out to discriminate different species in the jet. Two tunable UV lasers were used: one was an intense pump laser, and the other was a weak probe laser. The probe laser frequency was tuned to the electronic transition, normally the 0^0_0 band, of a particular species in the jet, and its fluorescence intensity was monitored as a measure of the ground state population, similar to FDIR spectroscopy. The frequency of the pump laser was scanned through the electronic transition, and depletions in the fluorescence intensity occurred when pump laser frequencies coincided with the electronic transitions of the same species monitored by the probe laser. Thus, the SHB spectrum was obtained as a fluorescence-dip spectrum similar to FDIR spectroscopy. The pump and probe laser beams were focused on the jet at 5 and 15 mm down stream of the nozzle, respectively, with $f =$ 500 mm lenses, and the delay time of the two lasers was set to 5.5 μs. The time delay (5.5 μs) and the distance (10 mm) between the pump and the probe lasers were set to discriminate an intense fluorescence signal and scattered light caused by the pump laser from the fluorescence signal monitored by the probe laser.

7HQ and 7HQ-$(CH_3OH)_n$ clusters were generated by a supersonic expansion of a 7HQ vapor seeded in a 5% mixture of CH_3OH/He at a total pressure of 3 atm. 7HQ was heated at 450 K to obtain a sufficient vapor pressure. The mixture was expanded into vacuum through a pulsed nozzle having an 800 μm orifice. The probe UV light was a second harmonic of a Nd:YAG laser (Spectra-Physiks INDI-50−10)-pumped dye laser (Lumonics HD-500 with DCM or Pyridine1 dye). The output power and the spectral resolution of the UV light were 5 μJ and 0.2 cm^{-1}, respectively. Fluorescence was collected by a lens and detected by a photomultiplier tube (Hamamatsu Photonics 1P28) after passing through a band-pass filter. The photocurrent from the photomultiplier tube was integrated by a boxcar integrator (Par model 4400/4420) connected with a microcomputer. A tunable IR light for FDIR spectroscopy was generated by a difference frequency mixing between a second harmonic of an injection-seeded Nd:YAG laser (Quanta Ray GCR 230) and the Nd:YAG laser-pumped dye laser (Continuum ND6000, DCM dye) with a $LiNbO_3$ crystal. The typical output power and the spectral resolution of the IR light were 0.4 mJ and 0.1 cm^{-1}, respectively. The pump UV laser light for UV−UV SHB spectroscopy was a second harmonic of the injection-seeded Nd:YAG laser (Quanta Ray GCR 230) laser-pumped dye laser(Continuum ND6000), and its typical output power was 0.3 mJ. Dispersed fluorescence spectra were measured with an $f = 250$ mm monochromator (Nikon G-250). 7HQ was purchased from Acros Organics and was used without purification.

Density functional theory calculations were carried out to analyze the structures and vibrations of 7HQ-$(CH_3OH)_n$. Fully optimized minimum-energy structures were computed at the B3LYP/6-31G(d,p) level without any constraints. Normal coordinate calculations to obtain the harmonic frequencies were carried out for each optimized structure at the same level. The calculated frequencies were multiplied by a scaling factor of 0.9565. The H-bond binding energies (D_e and D_0) were also calculated. The zero point energy (ZPE) correction was done by using the same scaling factor. The full counterpoise (CP) procedure was used to correct the binding energy for the basis set superposition error (BSSE).[36] The calculations were carried out using the Gaussian 98 program.[37]

III. Results and Discussion

A. S_1-S_0 LIF Spectrum. *1. 7HQ-$(CH_3OH)_1$.* First of all, it is necessary to mention the existence of two isomers for bare 7HQ, that is, cis- and trans-rotamers depending on the direction of the OH group with respect to the quinoline plane. As was reported in our previous paper, the laser induced fluorescence (LIF) intensity of the 0^0_0 band of cis-isomer is 6 times stronger than that of trans-isomer.[34] Furthermore, we found that the relative LIF intensities of the clusters of the trans-isomer are much weaker than those of the cis-isomer. Thus, we can safely assume that all the clusters observed here are due to *cis*-7HQ.

The S_1-S_0 LIF spectrum of 7HQ-$(CH_3OH)_1$ is presented in Figure 2. Two electronic transitions exhibiting different spectral features are observed in the lower frequency side of the 0^0_0 band of bare *cis*-7HQ at 30 843 cm^{-1}. One is located in the 30 100−30 300 cm^{-1} region, where the band origin occurs at 30 131 cm^{-1} with a few intermolecular vibrations in the higher

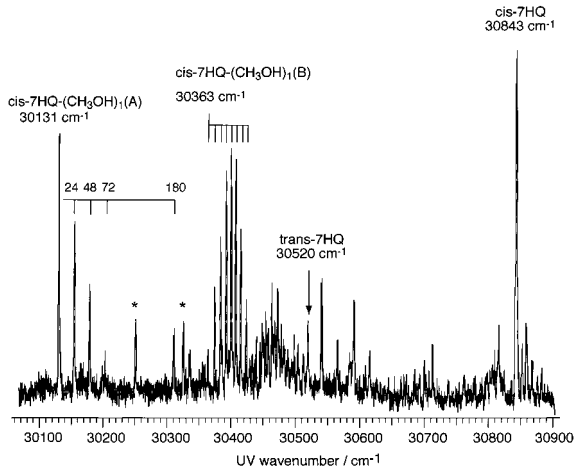

Figure 2. S_1-S_0 LIF spectrum of bare 7HQ and *cis*-7HQ-$(CH_3OH)_1$. Bands marked by asterisk are due to an impurity.

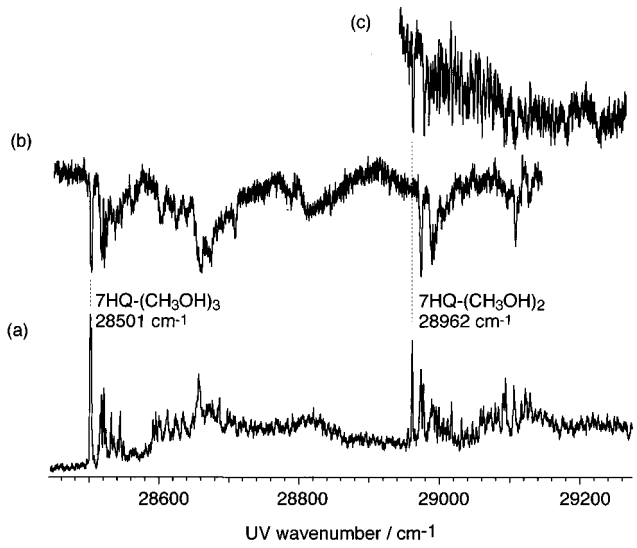

Figure 3. (a) S_1-S_0 LIF spectrum of 7HQ-$(CH_3OH)_2$ and -$(CH_3OH)_3$. (b) UV−UV SHB spectrum of 7HQ-$(CH_3OH)_3$, where the probe laser frequency is tuned to the band at 28 501 cm^{-1}. (c) UV−UV SHB spectrum of 7HQ-$(CH_3OH)_2$, where the probe laser frequency is tuned to the band at 28 962 cm^{-1}.

frequency side. The other transition is observed in the 30 360−30 450 cm^{-1} region, where a 10 cm^{-1} progression is seen starting from the band origin at 30 363 cm^{-1}. Lahmani et al. assigned the former to the transition of *trans*-7HQ-$(CH_3OH)_1$ and the latter to *cis*-7HQ-$(CH_3OH)_1$.[18] However, as will be discussed later, the two transitions are assigned to two different isomers of *cis*-7HQ-$(CH_3OH)_1$. We refer the former as *cis*-7HQ-$(CH_3OH)_1$(A), and the latter as *cis*-7HQ-$(CH_3OH)_1$(B), as indicated in Figure 2. The IR spectroscopic measurements and the DFT calculations for determination of those structures will be discussed later.

2. 7HQ-$(CH_3OH)_2$ and -$(CH_3OH)_3$. Figure 3a shows the S_1-S_0 LIF spectrum of *cis*-7HQ-$(CH_3OH)_2$ and -$(CH_3OH)_3$. There are two intense bands at 28 962 and 28 501 cm^{-1}, and their vibronic bands are seen in the 29 000−29 200 and 28 560−28 700 cm^{-1} regions, respectively. Lahmani et al. described that the bands observed in these regions might be due to the cluster of 7HQ involving two or three CH_3OH molecules, from the results of the methanol vapor pressure dependence of the band intensities.[18] To make more definitive assignment for these bands, we applied UV−UV spectral hole-burning (SHB) spectroscopy. Figure 3b,c shows the SHB spectra obtained by fixing the probe laser frequencies to the bands at 28 501 and 28 962 cm^{-1}, respectively. As seen in Figure 3b, when we monitored the band at 28 501 cm^{-1}, no depletion occurred at 28 962 cm^{-1}, which means that the species of the band at 28 501 cm^{-1} differs from that of the band at 28 962 cm^{-1}. As will be described later, we measured the FDIR spectra by monitoring the bands at 28 962 and 28 501 cm^{-1}, and assigned them to the 0^0_0 transitions of 7HQ-$(CH_3OH)_2$ and -$(CH_3OH)_3$, respectively.

The redshifts of the 0^0_0 band frequencies of 7HQ-$(CH_3OH)_2$ and -$(CH_3OH)_3$ relative to that of the *cis*-7HQ monomer are 1881 and 2342 cm^{-1}, respectively. These values are similar to those of 7HQ-$(H_2O)_n$, that is 1650 and 2072 cm^{-1} for $n = 2$ and 3, respectively.[19−21,34] Also, 7HQ-$(NH_3)_n$ exhibit very similar redshifts in electronic transition frequencies, that is, 1729 and 2045 cm^{-1} for $n = 2$ and 3, respectively.[22] Thus, all these results support our assignments of the 0^0_0 bands for 7HQ-$(CH_3OH)_2$ and -$(CH_3OH)_3$.

TABLE 1: Binding Energies of 7HQ-$(CH_3OH)_n$ at the B3LYP/6-31G(d,p) Level Calculation[a]

	E_{rel}[b]	D_e[c]	BSSE	ZPE[d]	D_0[e]
cis-7HQ-$(CH_3OH)_1$ (OH−N)	0	−3 102	1234	536	−1 332
cis-7HQ-$(CH_3OH)_1$ (OH−O)	105	−2 996	1061	491	−1 444
cis-7HQ-$(CH_3OH)_2$ (bridge)	0	−7 948	2641	1226	−4 081
cis-7HQ-$(CH_3OH)_2$ (ring)	1010	−6 937	2587	1162	−3 181
7KQ-$(CH_3OH)_2$ (bridge)	3308	−9 137	2751	1161	−5 225
cis-7HQ-$(CH_3OH)_3$ (bridge)	0	−13 771	3864	1648	−8 259
cis-7HQ-$(CH_3OH)_3$ (ring)	2001	−11 770	3358	1630	−6 782
7KQ-$(CH_3OH)_3$ (bridge)	2469	−15 800	4100	1561	−10 139

[a] In inverse centimeters. [b] Total energy relative to most stable isomers for each cluster size. [c] Difference between the potential minimum of cluster and the sum of that of components. [d] Scaled by a factor of 0.9565. [e] Energy difference including zero point energy ($D_0 = D_e$ + BSSE + ZPE).

B. IR Spectra and Structural Analysis. In this section, we present the FDIR spectra of the OH stretching vibrations of *cis*-7HQ-$(CH_3OH)_n$, obtained by fixing the UV frequencies to the corresponding bands shown in Figures 2 and 3. In addition, we present energy-optimized structures and simulated IR spectra obtained by DFT calculations, which are compared with the observed IR spectra. The calculated H-bond binding energies of *cis*-7HQ-$(CH_3OH)_{1-3}$ are listed in Table 1. The frequencies of the observed and the calculated OH stretching bands are listed in Table 2.

1. 7HQ-$(CH_3OH)_1$. Figure 4a,b shows energy-optimized structures of two isomers of *cis*-7HQ-$(CH_3OH)_1$ obtained by DFT calculations at the B3LYP/6-31G(d,p) level. The isomer shown in Figure 4a has the form in which the OH group of 7HQ acts as a proton donor. The other isomer shown in Figure 4b has the form in which the nitrogen site of 7HQ acts as a proton acceptor. The structures of the two isomers are quite similar to those of *cis*-7HQ-$(H_2O)_1$, reported in a previous paper,[34] and we refer them as "OH−O" and "N−HO", respectively. The calculated binding energies of the "OH−O" and the "N−HO" isomers are 1444 and 1332 cm^{-1}, respectively. Because of the small energy difference, the two isomers are expected to coexist in a supersonic jet.

Figure 5c,d shows the FDIR spectra obtained by monitoring the LIF bands at 30 131 and 30 400 cm^{-1} in Figure 2, respectively. For comparison, the position of the OH stretching vibration of gas-phase CH_3OH and the FDIR spectrum of bare *cis*-7HQ are shown in parts a and b of Figure 5, respectively. In parts c and d of Figure 5, two vibrations are observed, which are assigned to the OH stretching vibrations of either 7HQ or CH_3OH. Since the observed spectra exhibit different OH

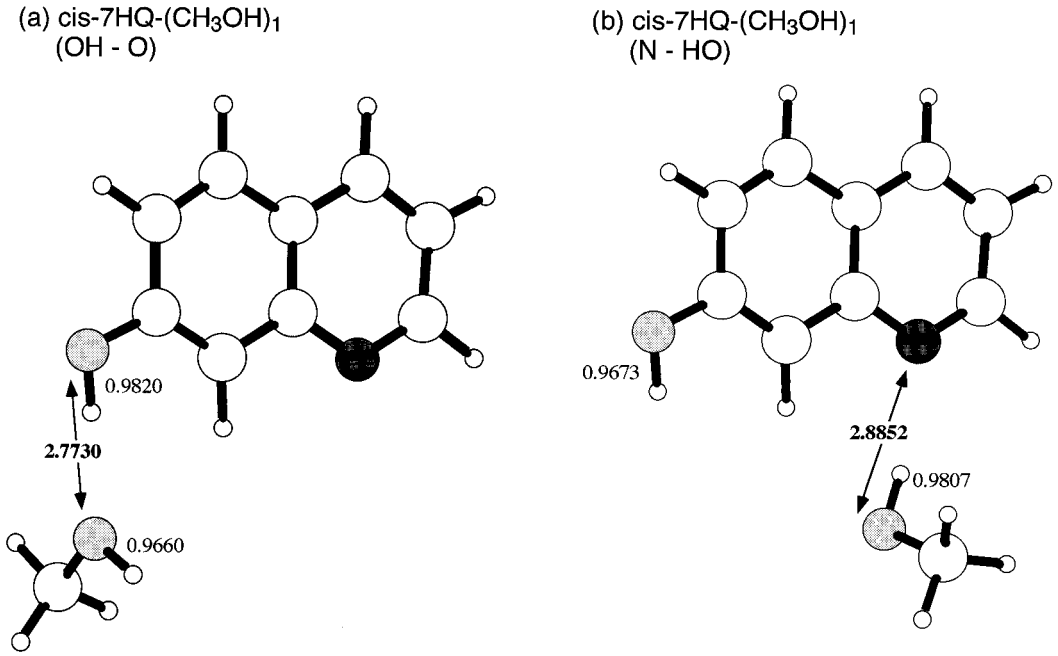

Figure 4. The energy-optimized structures of (a) *cis*-7HQ-$(CH_3OH)_1$(OH−O) and (b) *cis*-7HQ-$(CH_3OH)_1$(N−HO) obtained by the DFT calculations at the B3LYP/6-31G(d,p) level. The values indicate the OH bond length and the interatomic distance between O and O (N) in Å unit. The figures are drawn by using the MOLCAT program.[40]

TABLE 2: Observed and Calculated Frequencies (cm^{-1}) of OH Stretching Vibrations of *cis*-7HQ-$(CH_3OH)_n$ ($n = 1-3$)

	frequency		
	observed	calculated[a]	assignment
cis-7HQ	3650	3650	ν_{OH}
trans-7HQ	3659	3660	ν_{OH}
cis-7HQ-$(CH_3OH)_1$ (OH−O)	3686	3661	free $\nu_{OH}(CH_3OH)$
	3420	3363	H-bond ν_{OH}(7HQ)
cis-7HQ-$(CH_3OH)_1$ (OH−N)	3644	3646	free ν_{OH}(7HQ)
	3382	3374	H-bond $\nu_{OH}(CH_3OH)$
cis-7HQ-$(CH_3OH)_2$ (bridge)	3439	3421	H-bond ν_{OH}
	3323	3333	H-bond ν_{OH}
		3305	H-bond ν_{OH}
cis-7HQ-$(CH_3OH)_2$ (ring)		3522	
		3363	
		3175	
7KQ-$(CH_3OH)_2$ (bridge)		3324	
		3210	
		3151	
cis-7HQ-$(CH_3OH)_3$ (bridge)	3255	3218	H-bond ν_{OH}
	3205	3152	H-bond ν_{OH}
	3133	3049	H-bond ν_{OH}
	3078		H-bond ν_{OH}
cis-7HQ-$(CH_3OH)_3$ (ring)		3395	
		3257	
		3151	
7KQ-$(CH_3OH)_3$ (bridge)		3144	
		3055	
		2912	

[a] Each frequency is multiplied by a scaling factor of 0.9565.

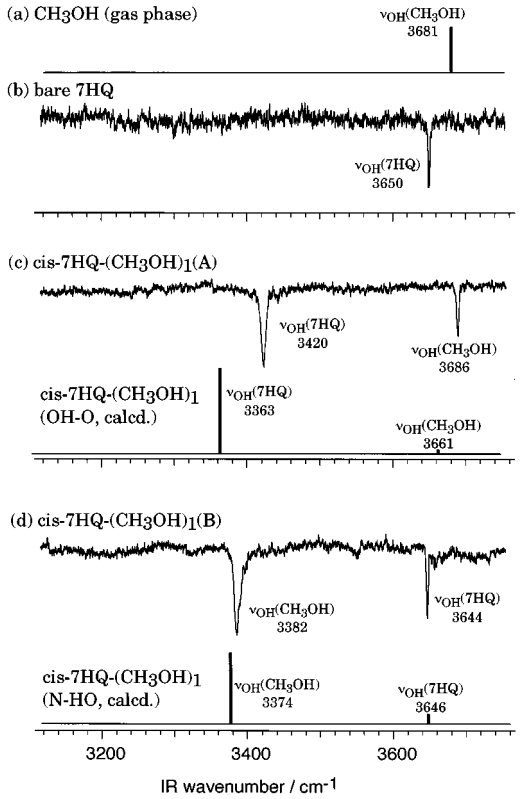

Figure 5. (a) Position of the OH stretching vibration of the gas-phase CH_3OH molecule. (b) FDIR spectrum of bare *cis*-7HQ obtained by monitoring the band at 30 843 cm^{-1}. (c), (d) FDIR spectra of *cis*-7HQ-$(CH_3OH)_1$(A) and *cis*-7HQ-$(CH_3OH)_1$(B) obtained by monitoring the bands at 30 131 and 30 400 cm^{-1}, respectively. Stick diagrams are the calculated IR bands of two isomers of *cis*-7HQ-$(CH_3OH)_1$(OH−O and N−HO) obtained by DFT calculations at the B3LYP/6-31G(d,p) level.

stretching vibrations, they are due to different isomers of *cis*-7HQ-$(CH_3OH)_1$, and we have to determine which species corresponds to which isomer in Figure 4. In the FDIR spectrum of *cis*-7HQ-$(CH_3OH)_1$(A) shown in Figure 5c, the higher frequency band (3686 cm^{-1}) is very close to the OH stretching vibration of CH_3OH in the gas phase (3681 cm^{-1}).[38] So this band is assigned to the OH stretch of the CH_3OH site acting as acceptor. The small redshift (5 cm^{-1}) is typical for the OH stretch vibration free from H-bond in many H-bonded clusters.[23,25] On the other hand, the intense band at 3420 cm^{-1}, which is redshifted by 230 cm^{-1} from the OH stretch of bare *cis*-7HQ (3650 cm^{-1}), is assigned to the H-bonded (or donor) OH stretching vibration of the 7HQ site. Thus, we conclude that *cis*-7HQ-$(CH_3OH)_1$(A) corresponds to the "OH−O" isomer shown in Figure 4a.

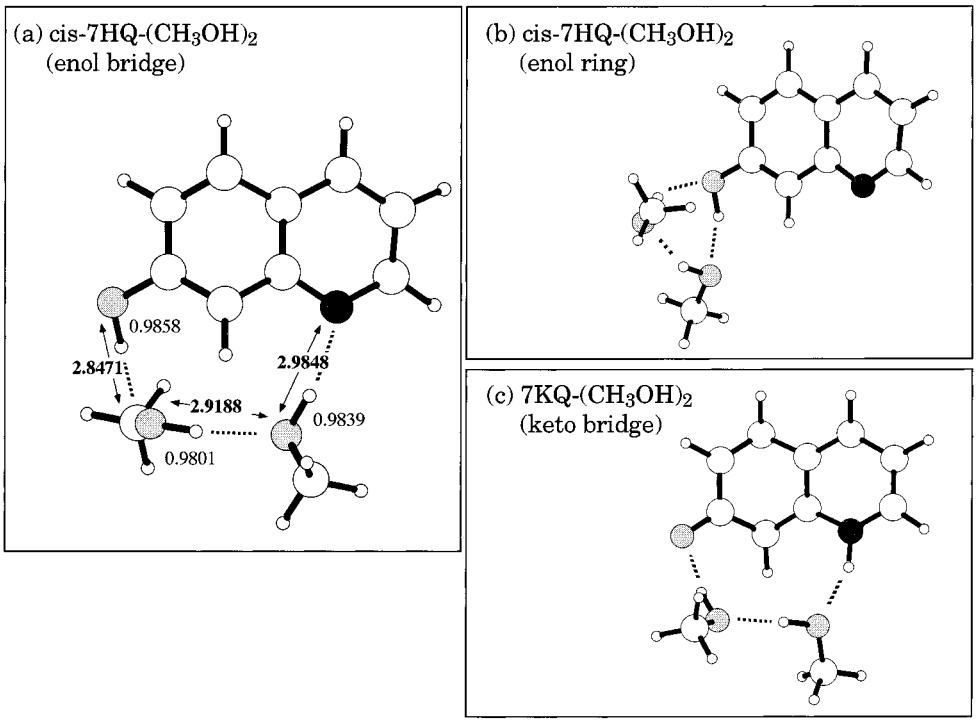

Figure 6. Energy-optimized structures of (a) *cis*-7HQ-$(CH_3OH)_2$ (enol bridge), (b) *cis*-7HQ-$(CH_3OH)_2$ (enol ring), and (c) 7KQ-$(CH_3OH)_2$ (keto bridge) obtained by DFT calculations at the B3LYP/6-31G(d,p) level. The inserted values are the OH bond lengths and the interatomic distances between O and O (N) atoms in Å unit.

In the FDIR spectrum of *cis*-7HQ-$(CH_3OH)_1$(B) shown in Figure 5d, it is noticed that the band at 3644 cm^{-1} is very close to the OH stretch of bare *cis*-7HQ. Thus, this band is assigned to the OH stretch of 7HQ free from H-bond by the similar reason described above. The band at 3382 cm^{-1} is assigned to the H-bonded OH stretch of CH_3OH, which is redshifted by 299 cm^{-1} relative to bare CH_3OH. This redshift is larger than that of *cis*-7HQ-$(H_2O)_1$(B) (256 cm^{-1}), which is consistent with the larger acidity of CH_3OH than H_2O.[34] Thus, the IR spectrum indicates that the nitrogen site of *cis*-7HQ is acting as proton acceptor, and CH_3OH as proton donor. That is, *cis*-7HQ-$(CH_3OH)_1$(B) is associated with the "N−HO" isomer shown in Figure 4b.

The stick diagrams in Figure 5c,d show the calculated IR bands for the energy-optimized structures shown in Figure 4. Though the calculated spectra do not give complete agreement with the observed one, they reproduce characteristic features of the H-bonded and free OH stretching vibrations with respect to the positions and intensities. As seen in Table 1, the calculated binding energies, D_0, of *cis*-7HQ-$(CH_3OH)_1$(A) and -(B), are almost equal, which also agrees with the observation, that is, comparable intensities of the two transitions in the LIF spectrum of Figure 2.

2. 7HQ-$(CH_3OH)_2$. Three possible isomers were obtained for 7HQ-$(CH_3OH)_2$ by DFT calculations at B3LYP/6-31G(d,p) level, which are shown in Figure 6a−c. The calculated binding energies of three isomers are also listed in Table 1. Figure 6a shows the "enol bridge" structure of *cis*-7HQ-$(CH_3OH)_2$, in which $(CH_3OH)_2$ is H-bonded to the OH hydrogen and to the nitrogen atom of *cis*-7HQ. This structure is the most stable one among the three isomers similar to that of 7HQ-$(H_2O)_2$ shown in our previous work[34] and by Bach et al.[20] Figure 6b shows the "enol ring" structure of *cis*-7HQ-$(CH_3OH)_2$, in which the OH group of *cis*-7HQ and two CH_3OH molecules form a cyclic H-bonding. This structure is very similar to that of 2-naphthol-$(H_2O)_2$[23] and phenol-$(H_2O)_2$.[25] The total energy of the enol ring structure is 1010 cm^{-1} higher than the enol bridge structure. Figure 6c shows the "keto bridge" structure of 7-keto-quinoline-(KQ)−$(CH_3OH)_2$, in which $(CH_3OH)_2$ is H-bonded to the amide

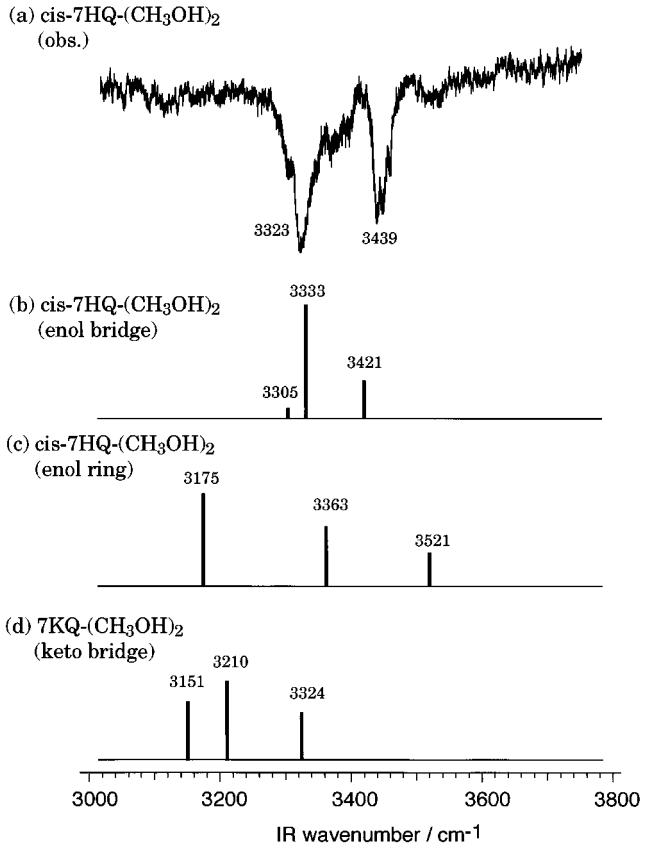

Figure 7. (a) FDIR spectrum of *cis*-7HQ-$(CH_3OH)_2$ obtained by monitoring the bands at 28 962 cm^{-1}. (b)−(d) Calculated IR spectra of three possible isomers of 7HQ-$(CH_3OH)_2$ obtained by DFT calculations at the B3LYP/6-31G(d,p) level.

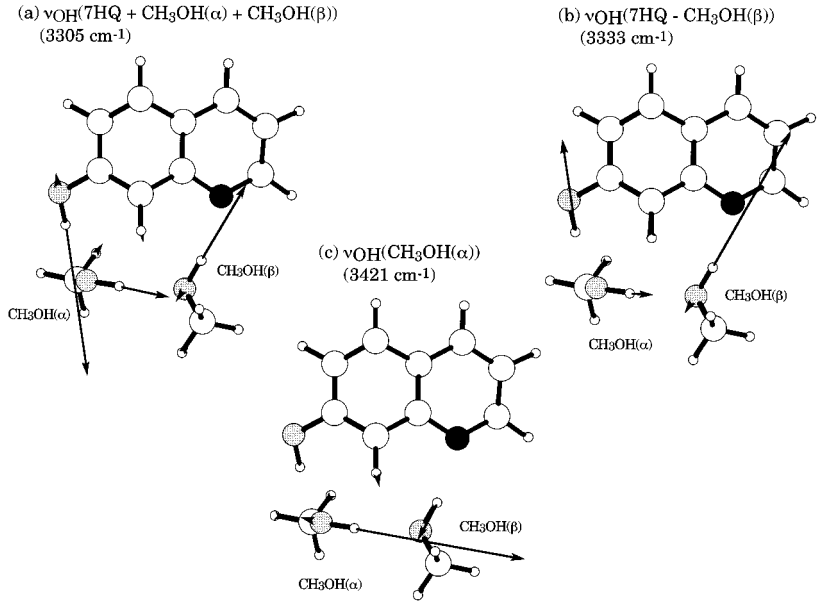

Figure 8. Normal modes and frequencies of the OH stretching vibrations of *cis*-7HQ-$(CH_3OH)_2$ (enol bridge) obtained by DFT calculations.

hydrogen and to the carbonyl oxygen of 7KQ, where 7KQ is the tautomer of *cis*-7HQ. The total energy of this structure is 3308 cm^{-1} higher than that of the enol bridge structure of *cis*-7HQ-$(CH_3OH)_2$. Thus, it is concluded that the enol bridge structure of *cis*-7HQ-$(CH_3OH)_2$ is the most stable isomer. It should be noted that the H-bond binding energy for the keto bridge form is 1144 cm^{-1} larger than that of the enol bridge form, though its total energy is less stable than that of the enol bridge form. Thus, the difference of the energies between *cis*-7HQ-$(CH_3OH)_2$ and 7KQ-$(CH_3OH)_2$ is mainly ascribed to the difference between 7HQ and 7KQ.

The enol bridge structure for the observed *cis*-7HQ-$(CH_3OH)_2$ is further supported by the analysis of the IR spectrum. Figure 7a shows the FDIR spectrum of *cis*-7HQ-$(CH_3OH)_2$ obtained by monitoring the LIF band at 28 962 cm^{-1}. In the spectrum, two intense broad bands appear at 3323 and 3439 cm^{-1}, which are assigned to the H-bonded OH stretching vibrations. Since no band occurs in the region of free OH stretching vibration (3650−3750 cm^{-1}), all the OH groups are thought to be H-bonded in the cluster. The simulated IR spectra of the enol bridge, enol ring, and keto bridge forms are shown as stick diagrams in Figure 7b−d. It is evident that the enol bridge spectrum reproduces the observed one very well. Thus, from the calculated binding energy and the agreement of the IR spectrum, we conclude that the structure of *cis*-7HQ-$(CH_3OH)_2$ is the enol bridge form as shown in Figure 6a.

Figure 8a−c shows the calculated normal modes of the OH stretch vibrations of the enol bridge form *cis*-7HQ-$(CH_3OH)_2$. It is seen that these vibrations are delocalized among all the OH groups. The lowest frequency mode (3305 cm^{-1}) is the "in-phase" motion of the OH stretch vibrations of 7HQ, $CH_3OH(\alpha)$ and $CH_3OH(\beta)$ so that this mode is denoted as "ν_{OH}(7HQ + $CH_3OH(\alpha)$+ $CH_3OH(\beta)$)". This mode has a weak IR absorption intensity as seen in Figure 7b. The mode with a frequency of 3333 cm^{-1} is the "out-of-phase" motion of the OH stretching vibrations of 7HQ and $CH_3OH(\beta)$, so that this mode is expressed as "ν_{OH}(7HQ-$CH_3OH(\beta)$)". The highest frequency mode (3421 cm^{-1}) is relatively localized on $CH_3OH(\alpha)$, so that it is expressed as "ν_{OH}($CH_3OH(\alpha)$)". It should be noted that such the delocalized motions are not observed in the "ring type" phenol-$(H_2O)_2$ or 2-naphtnol-$(H_2O)_2$ cluster, and are unique to clusters having "bridge type" structure. Similar motions were reported for the bridge type 2-pyridone-$(H_2O)_2$ cluster by Zwier's group.[39]

3. 7HQ-$(CH_3OH)_3$. Similar to 7HQ-$(CH_3OH)_2$, three stable forms were obtained for 7HQ-$(CH_3OH)_3$; the enol bridge, enol ring, and keto bridge forms. Figure 9a−c shows their energy-optimized structures obtained by DFT calculations at the B3LYP/6-31G(d,p) level. As shown in Table 1, the total energies of the enol ring and keto bridge forms are higher than that of the enol bridge form by 2001 and 2469 cm^{-1}, respectively. Thus, the enol bridge is the most stable isomer of 7HQ-$(CH_3OH)_3$. Figure 10a shows the FDIR spectrum of *cis*-7HQ-$(CH_3OH)_3$ obtained by monitoring the LIF band at 28 501 cm^{-1}. In the spectrum, three broad bands are overlapped in the region of 3000−3300 cm^{-1}. These bands are assigned to the H-bonded OH stretch vibrations whose frequencies are much more redshifted than those of *cis*-7HQ-$(CH_3OH)_2$. Sharp bands appearing below 3000 cm^{-1} are assigned to the CH stretch vibrations of CH_3OH molecules. Similar to the case of *cis*-7HQ-$(CH_3OH)_2$, the FDIR spectrum is compared with the calculated IR spectra of three possible isomers. The stick diagrams in Figure 10b−d show the calculated IR spectra of the enol bridge, the enol ring, and the keto bridge forms, respectively. Among them, it is clear that the calculated IR spectrum of the enol bridge form well reproduces the observed one. Thus, we conclude that the most probable structure of *cis*-7HQ-$(CH_3OH)_3$ is the enol bridge form, similar to that of *cis*-7HQ-$(CH_3OH)_2$.

C. ESPT Reaction of 7HQ-$(CH_3OH)_n$. *1. Size-Dependence.* As described in the Introduction, when 7HQ is excited to the S_1 state in alcoholic solution, a dual fluorescence (ultraviolet and visible) is observed. The visible fluorescence is attributed to the keto-tautomer (7KQ) generated by ESPT reaction. In the H-bonded clusters of 7HQ in the jet, a similar dual fluorescence was observed in 7HQ-$(NH_3)_{4-7}$ by Bach et al.,[22] indicating an occurrence of ESPT. In this section, we examine the ESPT reaction for 7HQ-$(CH_3OH)_n$ by observing the dispersed fluorescence (DF) spectra and discuss the size and structure effects on the ESPT reaction.

Before showing the DF spectra of each species, we should mention the presence of higher clusters in the electronic spectra. As seen in the LIF spectra of Figures 2 and 3, there exists broad background transition beneath the sharp bands. The broad background transition is thought to be due to larger size clusters.

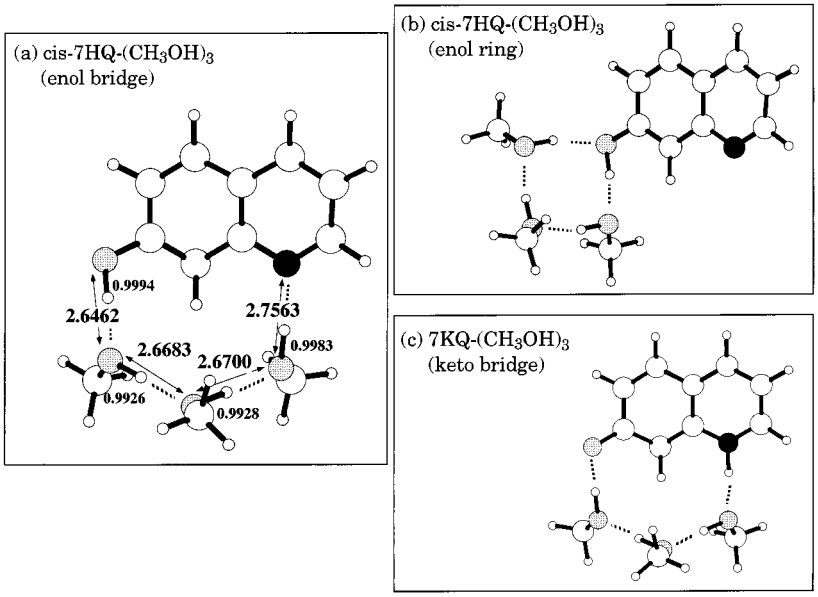

Figure 9. Energy-optimized structures of (a) *cis*-7HQ-$(CH_3OH)_3$ (enol bridge), (b) *cis*-7HQ-$(CH_3OH)_3$ (enol ring), and (c) 7KQ-$(CH_3OH)_3$ (keto bridge) obtained by the DFT calculations at the B3LYP/6-31G(d,p) level. The inserted values are the OH bond lengths and the interatomic distances between O and O (N) (bold) in Å unit.

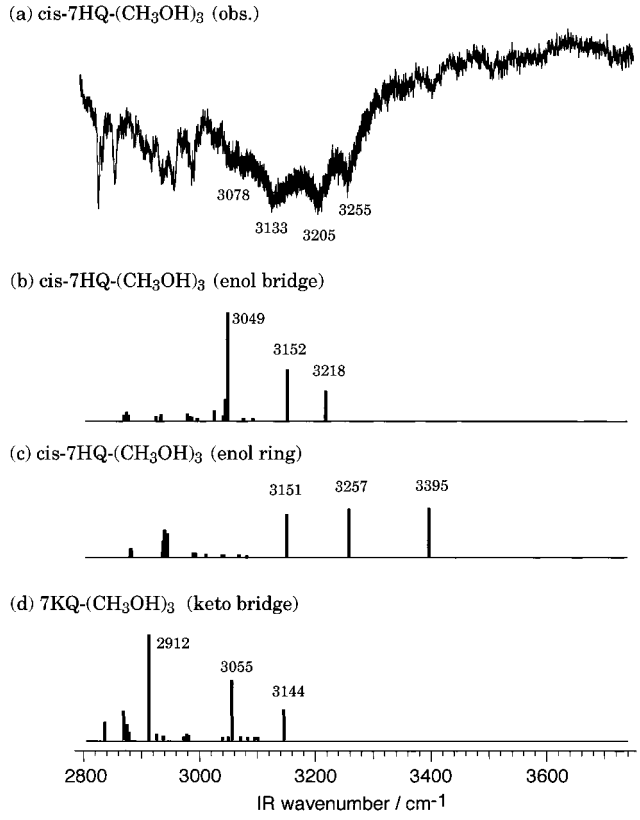

Figure 10. (a) FDIR spectrum of *cis*-7HQ-$(CH_3OH)_3$ obtained by monitoring the bands at 28 501 cm^{-1}. (b)−(d) Calculated IR spectra of three possible isomers of 7HQ-$(CH_3OH)_3$ obtained by DFT calculations at the B3LYP/6-31G(d,p) level.

To examine the ESPT reaction explicitly for each species, we have to discriminate the contribution of the larger size clusters. So, we observed two kinds of DF spectra: one is the spectrum obtained by exciting the sharp band, and the other is that obtained by detuning the UV frequency slightly from the sharp band. Finally, the former spectrum was subtracted by the latter. The DF spectra obtained with such a process are shown in Figure 11. Figure 11a−c shows the DF spectra of bare *cis*-7HQ and *cis*-7HQ-$(CH_3OH)_1$(A) and -(B), obtained by exciting their 0^0_0 bands. The spectral resolution of the monochromator was 300 cm^{-1}. The spectra represent a well resolved vibronic feature in the 25 000−31 000 cm^{-1} region without the visible emission. These results indicate that the ESPT reaction does not occur in bare *cis*-7HQ, *cis*-7HQ-$(CH_3OH)_1$(A) or -(B). Figure 11d shows the DF spectrum of *cis*-7HQ-$(CH_3OH)_2$, obtained by exciting the 0^0_0 band at 28 962 cm^{-1}. The spectrum was obtained with a monochromator resolution of 500 cm^{-1}. Similar to the case of *cis*-7HQ-$(CH_3OH)_1$, only UV emission is seen in the 22 000−29 000 cm^{-1} region with no visible emission. Though we also observed the DF spectrum by exciting the vibronic band at 29 429 cm^{-1} (0^0_0 + 467 cm^{-1}), no visible emission was observed. These results indicate that ESPT does not occur in the enol bridge *cis*-7HQ-$(CH_3OH)_2$, or that the reaction barrier may be much higher than 467 cm^{-1}.

Figure 11e shows the DF spectrum of *cis*-7HQ-$(CH_3OH)_3$, obtained by exciting the 0^0_0 band at 28 501 cm^{-1}. In addition to the UV emission in the 22 000−29 000 cm^{-1} region, a weak visible emission associated with the keto-form is clearly seen in the region of 16 000−20 000 cm^{-1}. Thus, we conclude that ESPT occurs at the zero-point level of enol bridge *cis*-7HQ-$(CH_3OH)_3$ in the S_1 state. We then extended our investigation to its vibronic band, and Figure 11f shows the DF spectrum obtained by exciting the band at 28 973 cm^{-1} (0^0_0 + 472 cm^{-1}). By comparing the spectra between parts e and f in Figure 11, we see that the intensity ratio of the visible to the UV emission is 3 times stronger for the vibronic band excitation than that of the origin excitation. Thus, if we assume that the fluorescence lifetimes are not different between the two levels, we can conclude that the ESPT rate constant becomes larger in the upper level.

2. Structure Effect. As described above, we obtained experimental evidence that the ESPT reaction occurs from the enol bridge *cis*-7HQ-$(CH_3OH)_n$ in S_1 and its critical size is $n = 3$. Hereafter, we discuss the difference of reactivity of ESPT between *cis*-7HQ-$(CH_3OH)_2$ and -$(CH_3OH)_3$ based on the structure of the clusters obtained by the DFT calculations.

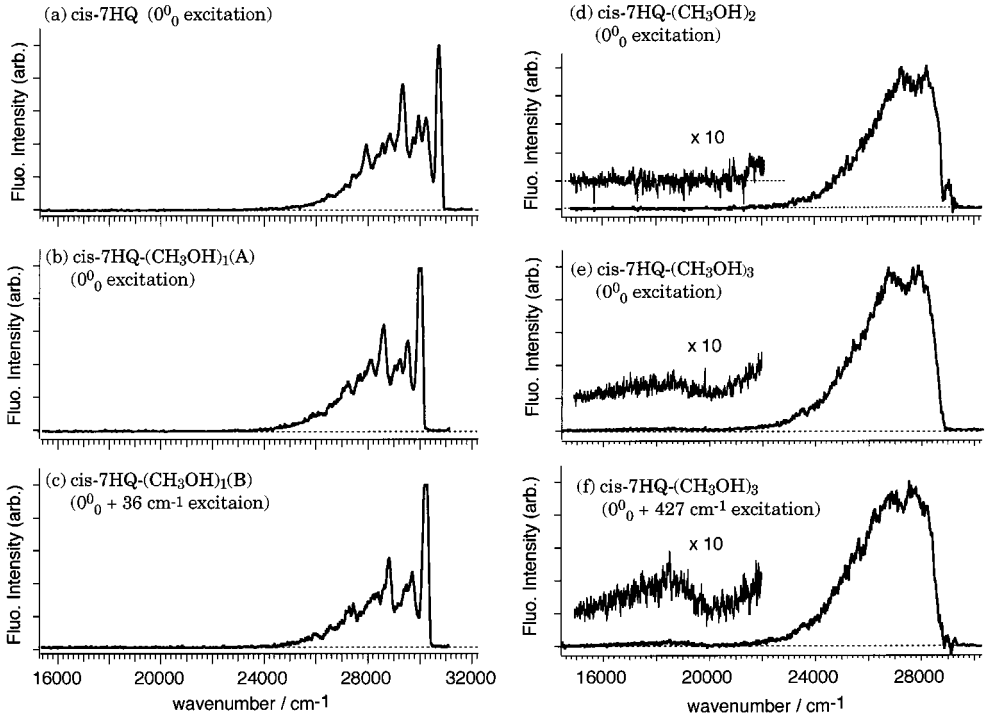

Figure 11. DF spectra obtained by exciting (a) the 0^0_0 band of bare *cis*-7HQ, (b) the 0^0_0 band of *cis*-7HQ-$(CH_3OH)_1$(A), (c) the $0^0_0 + 36$ cm^{-1} band of *cis*-7HQ-$(CH_3OH)_1$(B), (d) the 0^0_0 band of *cis*-7HQ-$(CH_3OH)_2$, (e) the 0^0_0 band of *cis*-7HQ-$(CH_3OH)_3$ (0^0_0 excitation), and (f) the $0^0_0 +$ 472 cm^{-1} band of *cis*-7HQ-$(CH_3OH)_3$. Spectral resolution of the monochromator is 300 cm^{-1} for parts a−c, and 500 cm^{-1} for parts d−f.

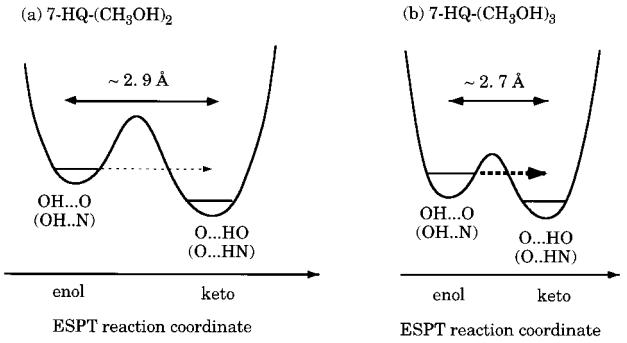

Figure 12. Schematic diagrams of the double minimum potential energy surface for the ESPT reaction corresponding to (a) *cis*-7HQ-$(CH_3OH)_2$ and (b) *cis*-7HQ-$(CH_3OH)_3$.

Since ESPT occurred from the zero-point level and its rate constant increased with the energy in enol bridge *cis*-7HQ-$(CH_3OH)_3$, the reaction may occur as a proton tunneling along the double minimum potential energy surface constructed with "enol" and "keto" forms, as shown in Figure 12. If it is the case, the proton tunneling probability depends on the height and width of the barrier which are governed by the O···O and O···N interatomic distances along which the proton transfer takes place. So we examined the O···O and O···N interatomic distances of the calculated enol bridge *cis*-7HQ-$(CH_3OH)_2$ and -$(CH_3OH)_3$ clusters shown in Figures 6a and 9a. We found that the average O···O and O···N interatomic distance is 2.92 Å in the former, while it is 2.69 Å in the latter. Thus, the average interatomic distance of *cis*-7HQ-$(CH_3OH)_3$ is 0.23 Å shorter than that of *cis*-7HQ-$(CH_3OH)_2$. Though the calculations were not performed for the S_1 state, we expect a similar situation for the clusters in the S_1 state. Thus, these results strongly suggest the higher proton tunneling probability of *cis*-7HQ-$(CH_3OH)_3$ than *cis*-7HQ-$(CH_3OH)_2$, which explains our observation of ESPT reaction in *cis*-7HQ-$(CH_3OH)_3$ but not in *cis*-7HQ-$(CH_3OH)_2$.

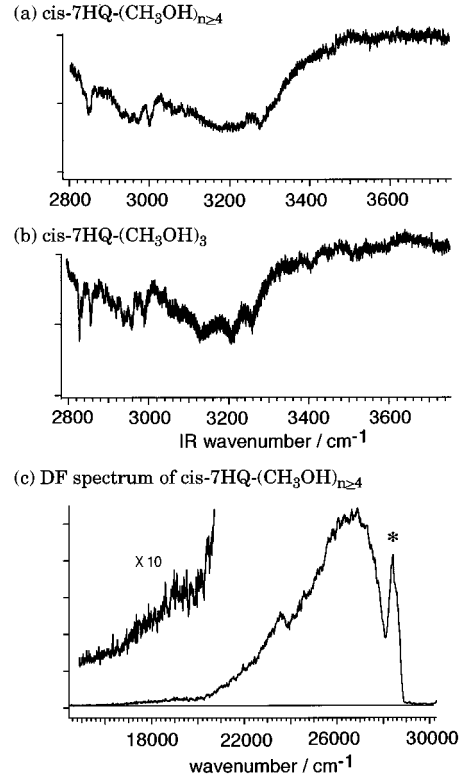

Figure 13. (a) FDIR spectrum of *cis*-7HQ-$(CH_3OH)_{n4}$ obtained by monitoring the broad LIF background at 28 487 cm^{-1}. (b) FDIR spectrum of *cis*-7HQ-$(CH_3OH)_3$ for comparison. (c) DF spectrum obtained by exciting the broad background at 28 487 cm^{-1}. The sharp peak at 28 480 cm^{-1} is due to scattered light which cannot be eliminated by the monochramator.

For the larger clusters, that is, 7HQ-$(CH_3OH)_{n\geq4}$, we have not carried out the calculation. However, the observed FDIR spectrum indicates a similar enol bridge type structure for them. Figure 13a shows the FDIR spectrum obtained by monitoring

the broad background whose position is 14 cm^{-1} to the lower frequency side of the 0^0_0 band of *cis*-7HQ-$(CH_3OH)_3$. We see that the IR spectrum is very similar to that of the enol bridge *cis*-7HQ-$(CH_3OH)_3$ shown in Figure 13b, suggesting a similar H-bonded structure for the monitoring species. Figure 13c shows the DF spectrum obtained after exciting this background absorption. As seen in the figure, the visible emission in the 16 000−20 000 cm^{-1} region is more distinct in the spectrum. Thus, the ESPT reaction is more enhanced in the larger cluster(s). The results indicate that in the larger clusters either the O···O and the O···N distances are shortened or the keto form is more stabilized in the S_1 state. Furthermore, in addition to the visible emission in the 16 000−20 000 cm^{-1} (yellow) region, we see another prominent feature in the 22 000−24 000 cm^{-1} (blue) region, which was also observed by Bach et al.[22] in the DF spectra of *cis*-7HQ-$(NH3)_{n>4}$ clusters, which is thought to be the emission from the 7HQ anion. At present, we have no clear evidence whether the blue emission is due to the 7HQ anion. It also should be noted that the intensity ratio of the visible emission to the UV emission for the observed clusters is much less than that reported for 7HQ in alcoholic solution[4,5] even for *cis*-7HQ-$(CH_3OH)_{n>4}$. Thus, though the critical size of ESPT was determined to be $n = 3$, there may be additional factors for this reaction to be promoted in solution, such as the stabilization of 7KQ potential energy surface with respect to that of 7HQ by the solvation of aromatic ring.

IV. Conclusion

In this work, we have investigated the H-bonded structures and the ESPT reaction in 7HQ-$(CH_3OH)_n$ clusters. By combining IR spectroscopy of the OH stretching vibrations of each species and the DFT calculations, their structures were determined. For 7HQ-$(CH_3OH)_1$, two isomers were found to exist: one has the structure in which the OH group of 7HQ acts as a proton donor, and the other has the structure in which CH_3OH forms a H-bond to the nitrogen site of 7-HQ as a proton donor. For 7HQ-$(CH_3OH)_2$ and -$(CH_3OH)_3$, their structures were determined to be of the enol bridge form. It was concluded that the ESPT reaction (keto−enol tautomerization) occurs as a proton tunneling reaction among the neighboring molecules in the enol bridge *cis*-7HQ-$(CH_3OH)_{n\geq 3}$. The critical size for ESPT is $n = 3$, and the O···O and O···N interatomic distances are the important factors for the ESPT reaction to occur.

Acknowledgment. The authors acknowledge Drs. A. Fujii, T. Maeyama, H. Ishikawa, and G. N. Patwari for their helpful discussion. T.E. also acknowledges Prof. M. Itoh for his suggestion and encouragement throughout this work. This work was partially supported by the Grant-in-Aids for Scientific Research (No. 12640483) by J.S.P.S. T.E. also acknowledges support from Sumitomo Foundation.

References and Notes

(1) Trieff, N. M.; Benson, B. R. *J. Phys. Chem.* **1965**, *69*, 2044.
(2) Mason, S. F.; Philip, J.; Smith, B. E. *J. Chem. Soc.* **1968**, *A*, 3051.
(3) Thistlethwaite, P. J. *Chem. Phys. Lett.* **1983**, *96*, 509.
(4) Itoh, M.; Adachi, T.; Tokumura, K. *J. Am. Chem. Soc.* **1983**, *105*, 4828.
(5) Itoh, M.; Adachi, T.; Tokumura, K. *J. Am. Chem. Soc.* **1984**, *106*, 850.
(6) Tokumura, K.; Itoh, M. *J. Phys. Chem.* **1984**, *88*, 3921.
(7) García-Ochoa, I.; Bisht, P. B.; Sánchez, F.; Martinez-Atáz, E.; Santos, L.; Tripathi, H. B.; Douhal, A. *J. Phys. Chem. A* **1998**, *102*, 8871.
(8) Chou, P. T.; Wei, C. Y.; Chris Wang, C. R.; Hung, F. T.; Chang, C. P. *J. Phys. Chem. A* **1999**, *103*, 1939.
(9) Lavin, A.; Collins, S. *Chem. Phys. Lett.* **1993**, *204*, 96.
(10) Lavin, A.; Collins, S. *Chem. Phys. Lett.* **1993**, *207*, 513.
(11) Lavin, A.; Collins, S. *J. Phys. Chem.* **1993**, *97*, 13615.
(12) Thistlethwaite, P. J.; Corkill, P. J. *Chem. Phys. Lett*. **1982**, *85*, 317.
(13) Nakagawa, T.; Kohtani, S.; Itoh, M. *J. Am. Chem. Soc.* **1995**, *117*, 7952.
(14) Kohtani, S.; Tagami, A.: Nakagaki, R. *Chem. Phys. Lett.* **2000**, *316*, 88.
(15) Wang, J.; Boyd, R. J. *Chem. Phys. Lett.* **1996**, *259*, 647.
(16) Fang, W. H. *J. Phys. Chem. A* **1999**, *103*, 5567.
(17) Coussan, S.; Meuwly, M.; Leutwyler, S. *J. Chem. Phys.* **2001**, *114*, 3524.
(18) Lahmani, F.; Douhal, A.; Breheret, E.; Zehnacker-Rentien, A. *Chem. Phys. Lett.* **1994**, *220*, 235.
(19) Bach, A.; Leutwyler, S. *Chem. Phys. Lett.* **1999**, *299*, 381.
(20) Bach, A.; Coussan, S.; Müller, A.; Leutwyler, S. *J. Chem. Phys.* **2000**, *112*, 1192.
(21) Bach, A.; Coussan, S.; Müller, A.; Leutwyler, S. *J. Chem. Phys.* **2000**, *113*, 9032.
(22) Bach, A.; Leutwyler, S. *J. Chem. Phys.* **2000**, *112*, 560.
(23) Matsumoto, Y.; Ebata, T.; Mikami, N. *J. Chem. Phys.* **1998**, *109*, 6303.
(24) Matsumoto, Y.; Ebata, T.; Mikami, N. *J. Mol. Struct.* **2000**, *552*, 257.
(25) Watanabe, T.; Ebata, T.; Tanabe, S.; Mikami, N. *J. Chem. Phys*. **1996**, *105*, 408.
(26) Iwasaki, A.; Fujii, A.; Watanabe, T.; Ebata, T.; Mikami, N. *J. Phys. Chem*. **1996**, *100*, 16053.
(27) Mitsuzuka, A.; Fujii, A.; Ebata, T.; Mikami, N. *J. Chem. Phys.* **1996**, *105*, 2618.
(28) Matsuda, Y.; Ebata, T.; Mikami, N. *J. Chem. Phys.* **2000**, *113*, 573.
(29) Ishikawa, S.; Ebata, T.; Mikami, N. *J. Chem. Phys.* **1999**, *110*, 9504.
(30) Guchhait, N.; Ebata, T.; Mikami, N. *J. Chem. Phys.* **1999**, *111*, 8438.
(31) Gruenloh, C. J.; Carney, J. R.; Arrington, C. A.; Zwier, T. S.; Fredericks, S. Y.; Jordan, K. D. *Science* **1997**, *276*, 1678 and references therein.
(32) Buchhold, K.; Reinmann, B.; Djafari, S.; Barth, H.-D.; Brutschy, B.; Tarakeshwar, P.; Kim, K. S. *J. Chem. Phys***. 2000**, *112*, 1844.
(33) Schmitt, M.; Jacoby, C.; Gerhards, M.; Unterberg, C.; Roth, W.; Kleinermanns, K. *J. Chem. Phys.* **2000**, *113*, 2995.
(34) Matsumoto, Y.; Ebata, T.; Mikami, N. *Chem. Phys. Lett.* **2001**, *338*, 52.
(35) Ebata, T.; Mizuochi, N.; Watanabe, T.; Mikami, N. *J. Phys. Chem*. **1996**, *100*, 546.
(36) Boys, S. F.; Bernardi, F. *Mol. Phys*. **1970**, *19*, 553.
(37) Frisch, M. J.; Trucks, G. W.; Schlegel, H. B.; et al. *Gaussian 98*, rev. A.2; Gaussian: Pittsburgh, PA, 1998.
(38) Herzberg, G. *Molecular Spectra and Molecular Structures III*; Van Nostrand Reinhold: New York, 1996.
(39) Florio, G. M.; Gruenloh, C. J.; Quimpo, R. C.; Zwier, T. S. *J. Chem. Phys.* **2000**, *113*, 11143.
(40) Tsutsui, Y.; Wasada, H. *Chem. Lett.* **1995**, 517.